RESEARCH

Transcriptomic and Physiological Analysis Reveal Melanin Synthesis-Related Genes and Pathways in Pacific Oysters (*Crassostrea gigas*)

Kunyin Jiang[1] · Chengxun Xu[1] · Hong Yu[1] · Lingfeng Kong[1] · Shikai Liu[1] · Qi Li[1,2]

Abstract

Shell color is one of the shell traits of molluscs, which has been regarded as an economic trait in some bivalves. Pacific oysters (*Crassostrea gigas*) are important aquaculture shellfish worldwide. In the past decade, several shell color strains of *C. gigas* were developed through selective breeding, which provides valuable materials for research on the inheritance pattern and regulation mechanisms of shell color. The inheritance patterns of different shell colors in *C. gigas* have been identified in certain research; however, the regulation mechanism of oyster pigmentation and shell color formation remains unclear. In this study, we performed transcriptomic and physiological analyses using black and white shell oysters to investigate the molecular mechanism of melanin synthesis in *C. gigas*. Several pigmentation-related pathways, such as cytochrome P450, melanogenesis, tyrosine metabolism, and the cAMP signaling pathway were found. The majority of differentially expressed genes and some signaling molecules from these pathways exhibited a higher level in the black shell oysters than in the white, especially after L-tyrosine feeding, suggesting that those differences may cause a variation of tyrosine metabolism and melanin synthesis. In addition, the in vitro assay using primary cells from mantle tissue showed that L-tyrosine incubation increased cAMP level, gene and protein expression, and melanin content. This study reveals the difference in tyrosine metabolism and melanin synthesis in black and white shell oysters and provides evidence for the potential regulatory mechanism of shell color in oysters.

Keywords *Crassostrea gigas* · Shell color · Melanin synthesis · Transcriptomic and physiological analysis · Mantle cell culture

Introduction

Molluscs shells often exhibit fabulous and variegated colors and elaborate patterns that influence consumer preference and increase their economic value (Barnard and De Waal 2006; Saenko and Schilthuizen 2021). Their shells are produced by the outer fold of the mantle (Boettiger et al. 2009) and grow linearly by adding new material to the growth edge in contact with the mantle (Williams 2017). Both shell growth and pigmentation are under neural control (Boettiger et al. 2009). Shell color has been proven to be heritable and influenced by environments and foods (Hoang et al. 2016; Xing et al. 2018, 2019). In the past decades, shell color has become a target trait in several molluscan breeding programs (Zhang et al. 2016; Xu et al. 2019a, b; Chen et al. 2020; Nie et al. 2020; Fu et al. 2021; Zhu et al. 2022). Several shell color strains or lines were developed through selective breeding, including *C. gigas* (Xu et al. 2019a, b), *Argopecten irradians* (Wang et al. 2020), *Meretrix meretrix* (Yue et al. 2015), and *Ruditapes philippinarum* (Yan et al. 2019).

The formation of different shell colors is influenced by three main reasons, including shell surface color, degree of coloration (coloration area, coloration depth), and shell structural or surface pattern (Williams et al. 2016; Irion et al. 2016; Williams 2017; Huang et al. 2021). The amount and distribution of pigments influence shell color polymorphism (Williams 2017). Three main types of pigments affect shell color: melanin, carotenoid, and porphyrin (Grant and Williams 2018). These pigments are

✉ Qi Li
qili66@ouc.edu.cn

1   Key Laboratory of Mariculture, Ministry of Education, Ocean University of China, Qingdao 266003, China

2   Laboratory for Marine Fisheries Science and Food Production Processes, Qingdao National Laboratory for Marine Science and Technology, Qingdao 266237, China

either directly acquired by food uptake or created by biosynthesis (Toews et al. 2017). Except for pigment-based shell colors, the microstructure of the calcium carbonate crystals that make up the shell also affects coloration (Saenko and Schilthuizen 2021). Structural colors are usually found in the interior of bivalves and gastropod shells and are produced in the nacreous layer (Saenko and Schilthuizen 2021).

Melanin is one of the most widely distributed pigments in nature, which is an important material basis for the formation of body color in animals (Williams et al. 2016). Melanin is a class of macromolecules with complex structure, high molecular weight, insoluble in water, acids, and organic solvents, and relatively stable physicochemical properties (Bandaranayake 2006). L-Tyrosine is a precursor of catecholamines and melanins, which is hydroxylated by tyrosinase to L-dihydroxyphenylalanine (L-DOPA) that oxidates further to Dopaquinone and subsequently melanin (Slominski and Paus 1994). L-Tyrosine and L-DOPA, in addition to being substrates and intermediates of melanogenesis, are also bioregulatory agents that regulate melanocyte functions (Slominski et al. 2004, 2012). The regulation mechanisms of melanin synthesis in mammals and teleosts are conserved and well-understood (Irion et al. 2016; Luo et al. 2021). It has been reported that human melanin synthesis is regulated by several pathways, including cAMP, Wnt, melanogenesis, and tyrosine metabolic signaling pathways (Slominski et al. 2004). There are four key regulatory pathways in fish melanocyte differentiation, development, and maturation, including SCF/KIT, Wnt/β-catenin, MAPK, and cAMP (Luo et al. 2021). Microphthalmia-associated transcription factor (*MITF*) is a key gene in the regulatory network of melanin synthesis, which is responsible for aggregating signals from all upstream pathways and mediating the synthesis of melanin by downstream tyrosinase family genes (Lister et al. 1999).

Pacific oysters (*Crassostrea gigas*) are important aquaculture bivalves that have been introduced and cultured in many countries (Guo 2009). Several shell color strains (black, white, golden, orange, and purple) of *C. gigas* have been developed through selective breeding, which exhibited fast growth and stable shell color (Xing et al. 2018, 2019; Xu et al. 2019a, b; Han et al. 2020). These strains provide valuable materials for research on pigment synthesis and the regulation mechanisms of shell color. Some previous works have revealed the inheritance patterns of shell color traits in *C. gigas* (Ge et al. 2014, 2015; Xing et al. 2019). However, previous studies on shell color only focused on the functional genes involved in melanin synthesis (Zhu et al. 2021; Li et al. 2022, 2023b), and the molecular mechanism of shell color formation is still limited.

In this study, we investigate the mechanism of melanogenesis and shell color formation in *C. giga* through transcriptomic and physiological analysis. The differences in tyrosine metabolism and melanin synthesis in black and white shell oysters were compared. We identified several key regulatory pathways and functional genes and further analyzed some important metabolites and enzymes from these pathways. In addition, the in vitro L-Tyrosine incubation assays using oyster mantle cells were performed to verify the cAMP-mediated melanogenesis pathway. The current study will provide important clues for understanding the mechanism of melanin synthesis and shell color formation in *C. giga*.

Materials and Methods

Oysters Maintenance and Sample Collection

Black and white shell color Pacific oysters (1 year in age) were used in this experiment. They are selectively bred strains and were cultured on a farm in Rongcheng, Shandong, China. Before the experiment, oysters were acclimatized in the laboratory for 7 days at a seawater temperature of 20 ± 0.3 °C and a pH of 8.1 ± 0.1. The oysters were divided into four groups: white shell control group (CW), black shell control group (CB), white shell tyrosine supplement group (TW), and black shell tyrosine supplement group (TB), respectively (Fig. 1A). There were three replicates for each group and 30 oysters in each replicate. During the experiment, TB and TW groups were fed *Chlorella vulgaris* and L-Tyrosine (10 mg/L) (Solarbio, Beijing, China) once a day. The control groups were fed *C. vulgaris* only. The seawater was changed daily before feeding. After 15 days of feeding, three individuals were randomly selected from each replicate for sampling. The edge mantle was collected, frozen in liquid nitrogen, and stored at -80 °C.

RNA Extraction and Library Construction

Total RNA was extracted from the collected edge mantle tissues using an RNA-easy Isolation Reagent (Vazyme, Nanjing, China). The quality and integrity of total RNA were detected using a 1% agarose gel, and the concentration was detected with a NanoPhotometer® spectrophotometer (IMPLEN, CA, USA). The quality of the library was evaluated using an Agilent Bioanalyzer 2100 instrument after the PCR products were purified using the AMPure XP system following the manufacturer's recommendations. Libraries were constructed using the NEBNext mRNA Library Prep Master Mix Set and Illumina HiSeq 2500 sequencing.
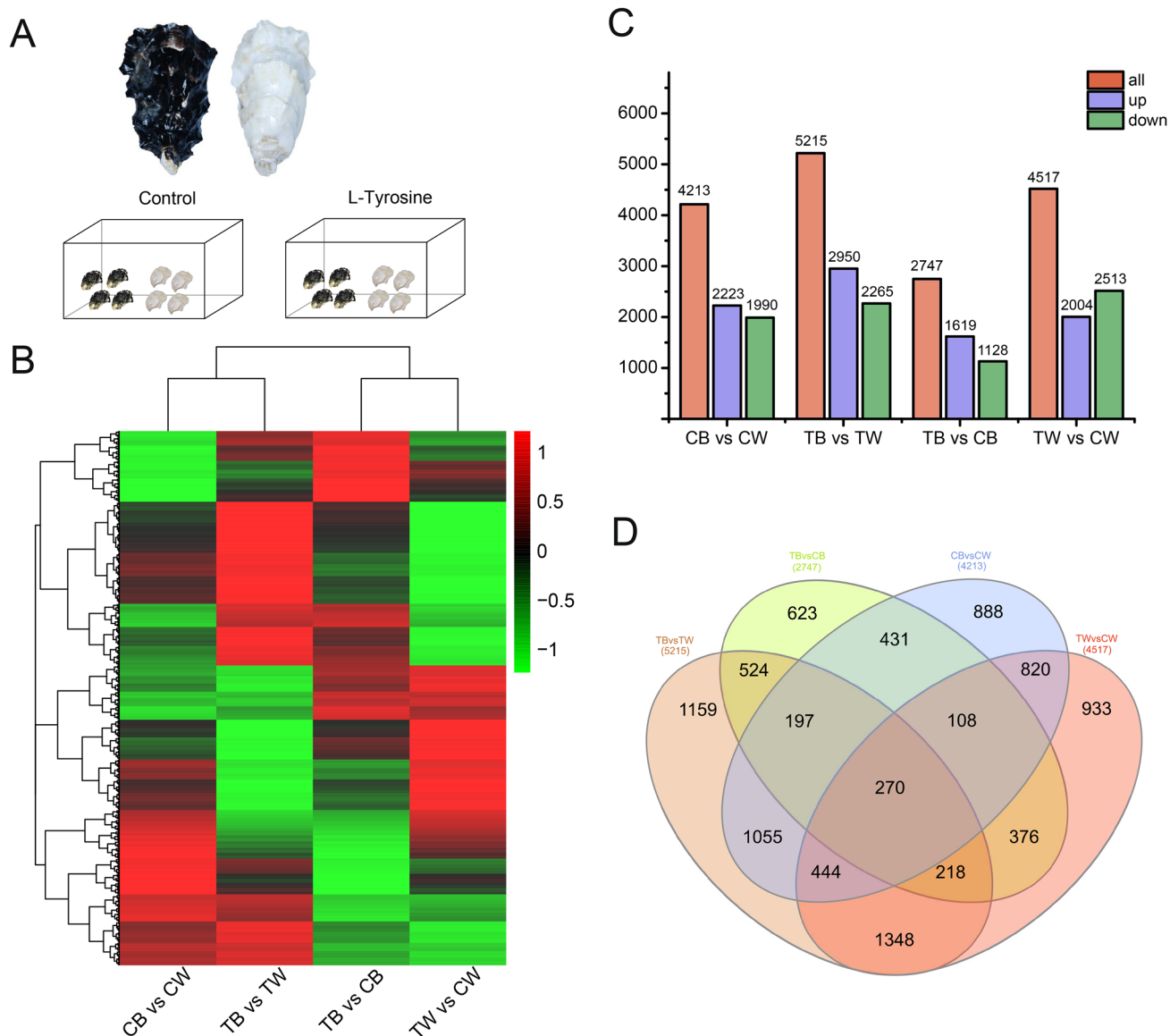
Fig. 1 Experimental design and gene expression in the edge mantel of black and white shell *C. gigas* before and after ʟ-Tyrosine supplements. **A** Experimental design. each group has three replicates ($n=30$). **B** The heatmaps present the expression patterns of DEGs in each comparison. **C** The numbers of DEGs in each comparison. **D** Venn diagram of DEGs in each comparison

Transcriptome Sequencing

The quality of raw reads was assessed using FastQC v0.11.8. The Q20, Q30, and GC content of the clean data were determined with fastp v0.20.1. All the downstream analyses used clean data. The reference genome (cgigas_uk_roslin_v1) index was constructed using Hisat2 v2.2.0. The number of reads that mapped to the reference genome was counted using FeatureCounts software. The fragments per kilobase per million fragments (FPKM) of each gene were calculated based on their length and the number of reads mapped to this gene. The abundance of genes was evaluated using the transcripts per million (TPM) method. Differential expression analysis was performed using DESeq2 R software. Genes with |Log2 Fold Change (log2FC)| > 1 and adjusted P value < 0.05 were considered differentially expressed genes (DEGs). ClusterProfiler v4.0.2 R package was used for Gene Ontology (GO) and Kyoto Encyclopedia of Genes and Genomes (KEGG) analysis.

Quantitative Real-time PCR (qPCR) Validation and Expression Analysis

Fifteen DEGs related to tyrosine metabolism and melanin synthesis were selected for qPCR validation and expression analysis. cDNA template was obtained by reverse

transcription PCR (RT-PCR) using Evo M-MLV RT Kit with gDNA Clean for qPCR kit (Accurate Biology, China). The primers were validated by PCR amplification and agarose gel electrophoresis. Amplification efficiency was calculated using a tenfold gradient dilution of the cDNA template with an equation: Efficiency $= 10^{(-1/\text{slope})}$. *Elongation factor Iα* (EFI-α) and *Glyceraldehyde 3-phosphate dehydrogenase* (GAPDH) were used as internal references for data analysis. qPCR experiments were performed on a Roche LightCycler 480 system (Roche, IN, USA) with SYBR Green Premix Pro Taq HS qPCR Kit (Accurate Biology, China). The $2^{-\Delta\Delta Ct}$ method was used to calculate the relative expression level of genes.

Tyrosinase Activity Assay

Tyrosinase activity was detected using a Tyrosinase activity assay Kit (Solarbio, Bejing, China). Extracting solution (1 mL) and 0.1 g sample was mixed and fully homogenized at 4 °C. The homogenates were centrifuged at 12,000 g for 20 min to obtain supernatant. Sample supernatant (20 μL) and Reagent I were added to a 96-well plate and recorded the absorbance wavelength (A1) at 475 nm at 10 s. Then the 96-well plate was placed in an incubator (25 °C) for 30 min and the absorbance wavelength (A2) at 475 nm was recorded. Tyrosinase activity was calculated according to the manufacturer's protocol.

Ferrous Sulfate Melanin Staining

Ferrous sulfate melanin staining was carried out with a ferrous sulfate staining kit (Leagene, China). After dewaxing, the sections of the oyster edge mantle were stained with ferrous sulfate for 1 h and washed with ultrapure water for 4 min 3 times. Then, the sections were stained with acidic potassium ferricyanide solution for 30 min and washed with ultrapure water for 4 min 3 times. The samples were counterstained with Eosin B (Sangon, China). After washing, samples were observed under a microscope (Olympus Corporation, Japan).

cAMP Measure Assay

A Mollusc cAMP ELISA Kit (GenScript, China) was used to measure cAMP. Samples and PBS (pH 7.4) with a weight ratio of 1:9 were fully homogenized using a low-temperature grinder and centrifuged at 3000 rpm for 20 min to obtain supernatant. Sample supernatant (50 μL) was added to 96-well plates (pre-coated with the antibody), and then the biotin-labeled antigen (50 μL) was added to wells and incubated at 37 °C for 30 min. The plate was washed with PBST 5 times, and then avidin-Horseradish Peroxidase (HRP) (50 μL) was added to wells and incubated at 37 °C

for 30 min. After washing with PBST 5 times, the developers A (50 μL) and B (50 μL) were added to wells for 10 min (protect from light). Finally, a stop solution (50 μL) was added to wells and the absorbance at 450 nm wavelength was measured using a microplate reader (BioTek, USA).

ELISA Assay

The Shellfish ELISA Kits of Melanin, Dopamine (DA), adrenaline (NA), and Norepinephrine (EPI) (NJJCBIO, China) were used to measure melanin, DA, NA, and EPI, respectively. Physiological saline was added to the sample with a weight ratio of 9:1. Samples were fully homogenized and centrifuged at 3000 g and 4 °C for 10 min. Sample supernatant (10 μL) and sample dilution (40 μL) were added to 96 plates. Then all wells were added 100 μL of HRP-labeled detection antibody and incubated for 60 min at 37 °C. After washing 5 times using wash solution, each well was added 50 μL of substrate A and B, respectively, and incubated for 15 min at 37 °C (protect from light). Finally, 50 μL of stop solution was added to each well and the OD value at 450 nm was recorded using a microplate reader (BioTek, USA).

Mantle Cells In Vitro Culture and ʟ-Tyrosine Treatment

In this study, oyster mantle cells were cultured for ʟ-Tyrosine treatment assay (Potts et al. 2020; Li et al. 2021a). Before the experiment, oysters were cleaned and sustained with filtered seawater containing Penicillin (100 U/mL) streptomycin (100 μg/mL), and gentamicin (50 μg/mL) under a UV lamp for 2 h. Oysters mantle tissues were collected and washed 6 times with PBS, exposed under a UV lamp for 30 min, then washed 6 times using a primary medium containing M199 and L15 medium (V:V = 1:1, pH 7.2–7.4), Penicillin (100 U/mL) streptomycin (100 μg/mL), and gentamicin (50 μg/mL). After washing, the mantle tissues were cut into minced meat with sterile scissors and cultured with the primary medium supplemented with 5% fetal bovine serum in a 12-well plate at 27 °C. After 48 h, a large number of cells migrated from the tissue. For treatment with ʟ-Tyrosine, ʟ-Tyrosine was added into the medium with final contractions of 0, 2, 10, 50, 100, and 500 μM for 16 h. Then the cultured cells were washed with PBS and collected for analysis. As above described methods, qPCR was carried out and tyrosinase activity, melanin content, cAMP, DA, NA, and EPI levels were detected.

Western Blot Analysis

For western blot analysis, the crude protein was extracted from the collected samples using RIPA lysis buffer

(Beyotime, China) containing PMSF (1 mM) (Beyotime, China). The concentration of crude protein was detected using a BCA Protein Concentration Assay Kit (Beyotime, China) and degenerated at 98 °C for 10 min. The samples with an amount of protein (30 μg) were separated by 10% SDS-PAGE and transferred to PVDF membranes under 200 mA for 70 min. The PVDF membranes were blocked with 5% skim milk for 2 h and incubated with antibodies against cAMP-responsive element binding protein (CREB) (1:2,000, ABclonal, China), Protein Kinase cAMP-dependent protein kinase regulator (PRKAR) (1:2,000, ABclonal, China), MITF (1:2,000, ABclonal, China), Tyrosinase (TYR) (1:1,000) (Li et al. 2023a), Tyrosinase related protein (TYRP) (1:1,000) (Li et al. 2023a), and GAPDH (1:2,000, ABclonal, China) for 14 h. After incubation, the PVDF membranes were washed three times with TBST for 10 min and then incubated with HRP-conjugated Goat Anti-Rabbit IgG (1:5,000, ABclonal, China) for 2 h. The immune-reactive protein bands were detected using an ECL chemiluminescence detection reagent (Vazyme, Nanjing, China).

Statistical Analysis

All the data were presented as mean $\pm$ SD and were analyzed by SPSS 20.0. The one-way analysis of variance (ANOVA) was employed to test for differences, and the Tukey post-hoc test was used to determine differences. The differences were considered statistically significant at $P < 0.05$ (*) and $P < 0.01$ (**).

Results

Transcriptome Sequencing and Assembly

In this study, 12 cDNA libraries were constructed. The raw reads were submitted to NCBI with an accession number PRJNA900369. Approximately 502.5 million clean reads were filtered from 12 libraries resulting in a total of 75.4G clean base (Table S1). The abundances of all genes were normalized and calculated using transcripts per million (TPM) values. Principal components analysis (PCA) showed that samples from the same group were clustered together (Fig. S1). Correlations among those samples varied from 0.83 to 0.99. Hierarchical cluster analysis showed a similar result to the PCA (Fig. S1).

DEGs and Expression Patterns Analysis

The heat maps of all DEGs were constructed to characterize the global expression profiles in four groups (Fig. 1B). Overall, The CB vs. CW group has a closer DEGs expression profile to TB vs TW, and TB vs. CB has a closer DEGs

expression profile with TW vs. CW comparisons. The number of DEGs in four comparisons is presented in Fig. 1C. The TB vs. TW comparison showed the highest number of DEGs (5215) and the TB vs. CB comparison had the lowest number of DEGs (2747) (Fig. 1C). The TW vs. CW group exhibited more DEGs than the TB vs. CB. A Venn diagram showed the shared and specific DEGs in those four comparisons (Fig. 1D).

Some genes related to pigment synthesis exhibited a higher expression level in the black shell *C. gigas* than the white, such as *TYR, TYRP, Tyramine beta-hydroxylase-like* (*TBH*)*, Dopamine beta-hydroxylase* (*DBH*), *5-hydroxytryptamine receptor 4-like* (*HTR4*), *Atrial natriuretic peptide receptor 1* (*ANPRA*), *Melanocortin receptor 4* (*MC4R*), *Corticotropin-releasing factor receptor 2 isoform X4* (*CRHR2*), *eIF-2-alpha kinase GCN2*, *Calmodulin* (*CALM*), etc. (Table S2). After L-Tyrosinase feeding, several genes were upregulated in black shell *C. gigas* compared to the white, including *TYRP1, TYRP2*, *DBH*, *Vacuolar protein sorting-associated protein 13A-like* (*VPS13*), *Bone morphogenetic protein 2-A* (*BMP2*), *Aromatic-L-amino-acid decarboxylase* (*DDC*), and *Multidrug resistance-associated protein 4-like* (*ABCC4*) (Table S2).

GO Enrichment Analysis

GO enrichment analysis was performed with DEGs from each group. The top 30 GO terms were presented in Fig. S2. The CB vs. CW and TB vs. TW groups shared GO terms including monoamine transmembrane transporter activity, endonuclease activity, nucleoside transmembrane transporter activity, and positive regulation of protein K63-linked ubiquitination. In the TB vs. CB group, DEGs enriched GO term mainly involved in amino acid metabolism, biosynthesis, and oxidoreductase activity, such as aromatic amino acid family metabolic process, primary amino compound biosynthetic process, serotonin biosynthetic process, tyrosine catabolic process, and oxidoreductase activity.

KEGG Enrichment Analysis

The top 30 KEGG pathways in these four groups are selected and presented in Fig. 2 (left). Several pigmentation-related pathways were found in the CB vs. CW group, including Tyrosine metabolism, Melanogenesis, Retinol metabolism, and cAMP signaling pathway. After L-Tyrosine supplements, more pigmentation and amino acid metabolism-related pathways were found in the TB vs. TW group compared to the CB vs. CW group, including Cytochrome P450, Steroid hormone biosynthesis, Betalain biosynthesis, Tyrosine metabolism, Isoquinoline alkaloid biosynthesis, cAMP signaling pathway, and Melanogenesis. Besides, compared to TW vs. CW, more
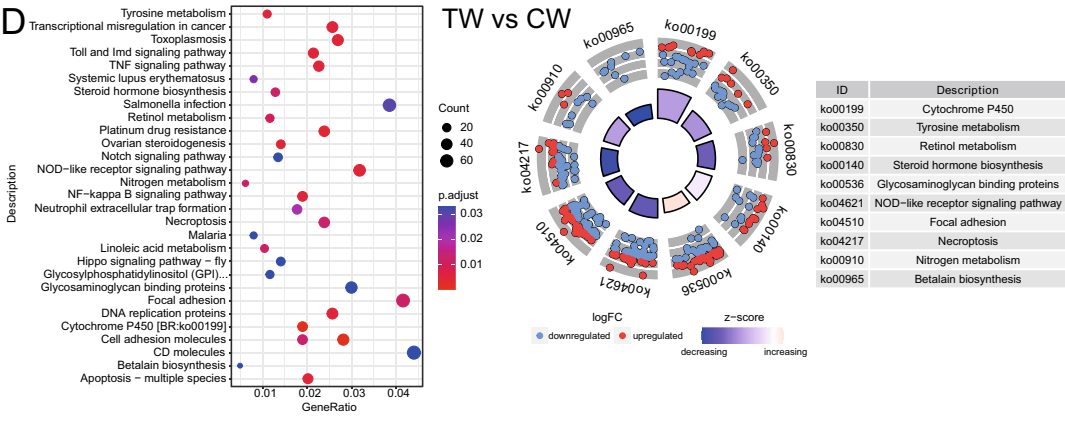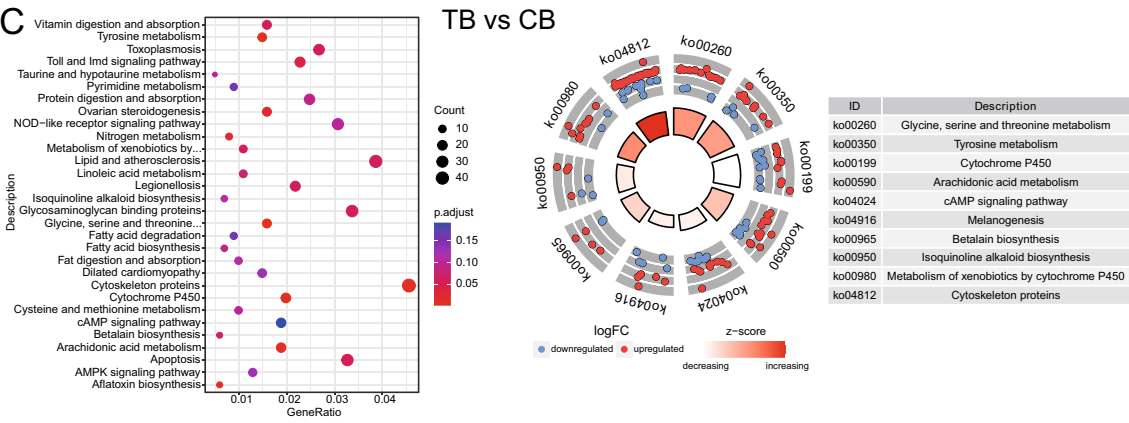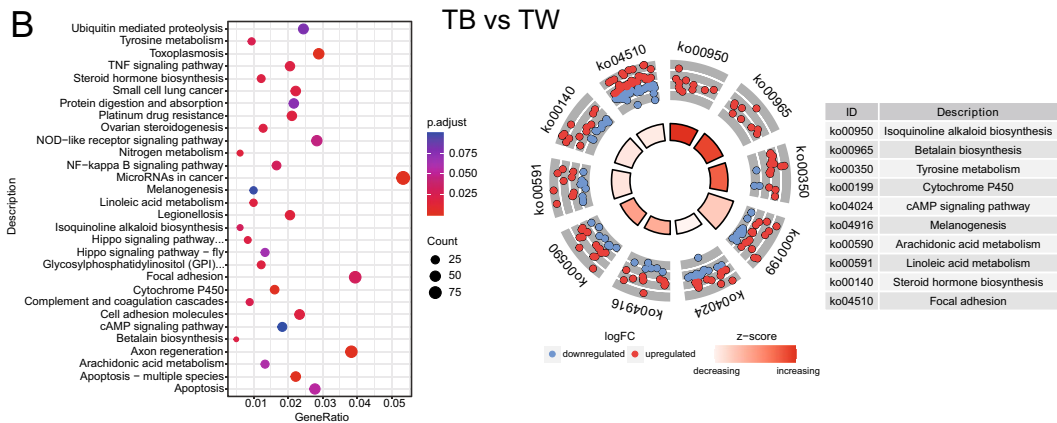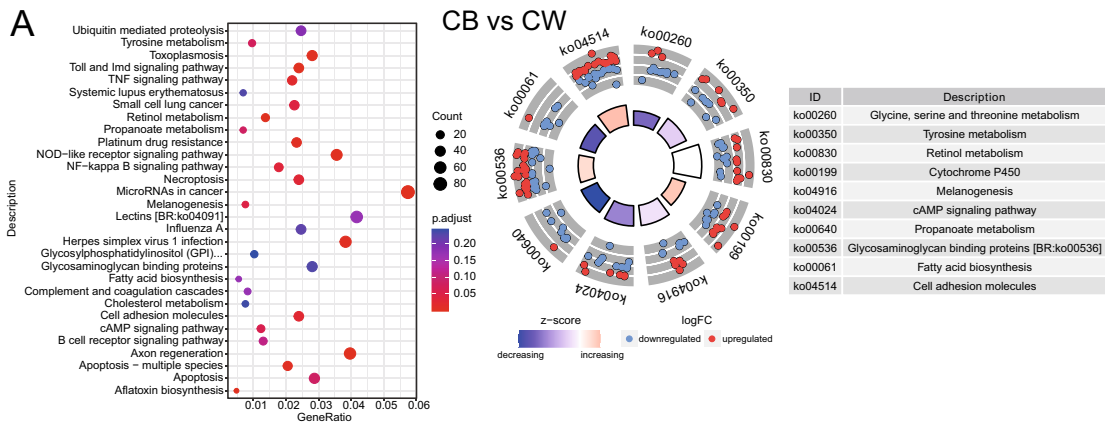
◄**Fig. 2** KEGG enrichment analysis. The top 30 KEGG and circle maps of **A** CB vs. CW, **B** TB vs. TW, **C** TB vs. CB, and **D** TW vs. CW comparisons. Several pathways involved in melanin synthesis were marked in red. Ten interested pathways were selected from each group to perform the circle map analysis (right). Most DEGs in TB vs. TW and TB vs. CB comparisons were upregulated

metabolism, biosynthesis, and pigmentation-related pathways were enriched in the TB vs. CB group, such as glycine, serine and threonine metabolism, Arachidonic acid metabolism, Metabolism of xenobiotics by cytochrome P450, Cysteine and methionine metabolism, Isoquinoline alkaloid biosynthesis, cAMP signaling pathway. The circle Maps were plotted using 10 interested pathways from each group, in which most of the DEGs exhibited an upregulated expression in TB vs. TW and TB vs. CB comparisons (Fig. 2, right).

Correlation Analysis of Selected Pathways and DEGs

To clarify the relationship in these pigmentation-related pathways, we performed a Gene-Concept Network analysis using DEGs from the selected pathways. In the CB vs. CW group, Tyrosine metabolism, Melanogenesis, Wnt signaling pathway, and cAMP signaling pathway were selected, and their interactions and key genes were presented in Fig. 3A. In the TB vs. TW group, seven pigmentation-related pathways were employed to conduct correlation analysis (Fig. 3B). As a result, the Melanogenesis pathway plays a central role in these processes. Some important genes involved in tyrosine metabolism and pigment synthesis were presented.

The global expression profiles of all DEGs from the cAMP signaling pathway, Tyrosine metabolism, and Melanogenesis were presented with a heatmap (Fig. S3). The expression profiles of 30 representative DEGs were shown in Fig. 4. DEGs from the cAMP signaling pathway, such as *HTR-8996, HTR-0084, MC4R ANPRA-8111,* and *ADCY1,* were expressed more abundantly in the black shell oysters (CB) than in the white shell oysters (CW). DEGs from Tyrosine metabolism and Melanogenesis pathway also showed a significantly higher expression in the black than in the white, including *DBH-1753, DBH-3978, TBH-2404, CALML3-8357, MITF, TYRP-6503,* and *TYRP-2218*. After feeding with L-Tyrosine, several Tyrosine metabolism and Melanogenesis rate-limiting enzymes presented an upregulated expression in the black compared to a downregulated or insignificant change in the white, including *DBH-0867, DDC-9411, DDC-0937, TYRP1-4830, TYRP-8244, TYRP2-4040*, and *TYRP1-2956*.

qPCR Validation

To validate the accuracy of RNA-seq data, qPCR analysis was performed using 15 interested DEGs. Table S3 contains a list of the specific primers used in this experiment. Primer amplification efficiencies ranged from 0.83 to 1.20. The fold change values of these DEGs detected by qPCR and RNA-seq are shown in Table 1. The qPCR results are consistent with the RNA-seq results.

Tyrosinase Activity Analysis

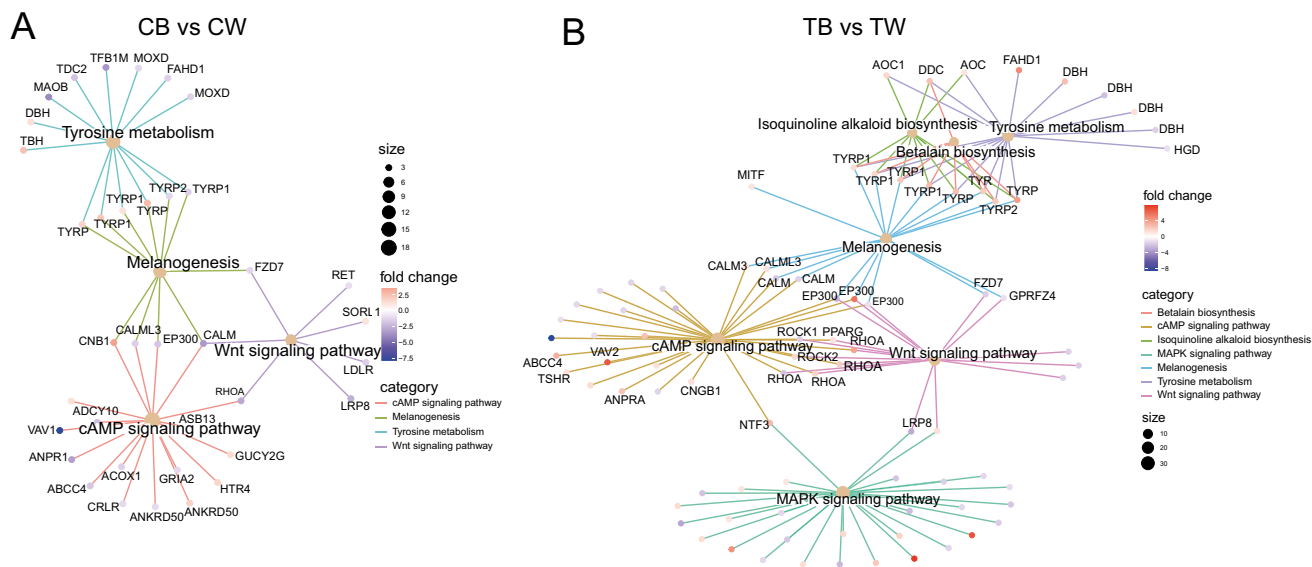Based on the results of the transcriptome, we found a difference in tyrosine metabolism between black and white shell

Fig. 3 Correlation analysis of tyrosine metabolism and melanin synthesis-related pathways and DEGs. **A** Four selected pathways from CB vs. CW group. **B** Seven selected pathways from TB vs. TW group. The color of DEGs presents fold changes of DEGs, red indicates upregulated, and blue represents downregulated
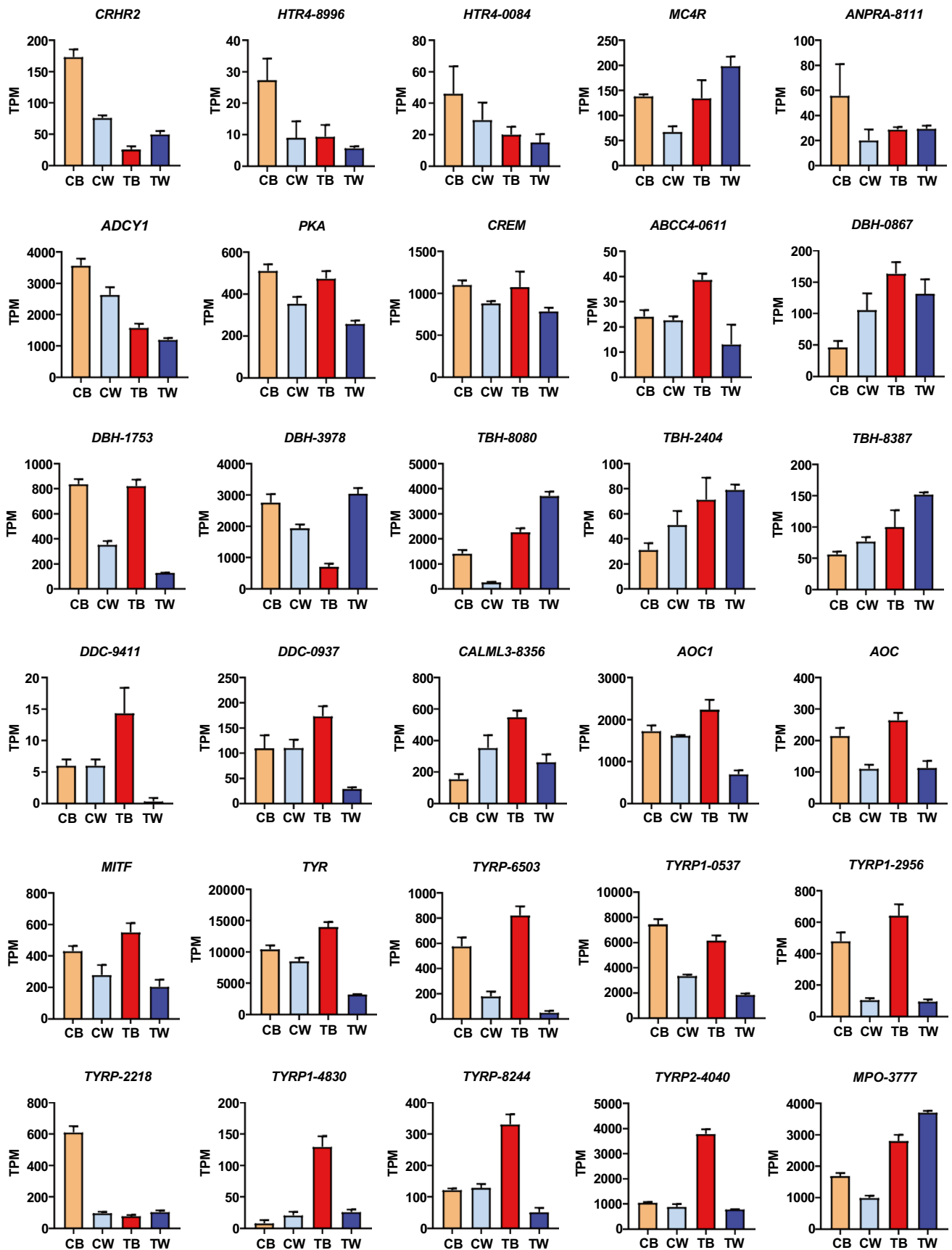
◀**Fig. 4** The expression profiles of representative genes from cAMP, Tyrosine metabolism, and Melanogenesis pathway. Most of these genes exhibited a higher TPM value in the black shell oysters than in the white. Most of these genes were upregulated in the black shell oysters after L-Tyrosine feeding

oysters. Then we compared the tyrosinase activity between black and white shell oysters. The tyrosinase activity was higher in black shell oysters than in the white ($P < 0.05$), but the difference was not significant (Fig. 5A). Noticeably, after L-Tyrosinase feeding, the activity of tyrosinase significantly increased in the black ($P < 0.05$) while that increased but was not significant in the white shell oysters.

Melanin Determination and Ferrous Sulfate Staining

The concentration of melanin was significantly higher in black shell oysters than in white shell oysters ($P < 0.05$) (Fig. 5B). After L-Tyrosine supplements, melanin highly increased in the black shell oysters ($P < 0.05$) but that change was not significant in white shell oysters. The oyster edge mantle has threefold, outer fold, middle fold, and inner fold. The ferrous sulfate staining showed clearly the distribution of melanin in oyster mantles. As is shown in Fig. 5C, melanin was only distributed in the part of the middle fold epidermis of white shell oysters, while in the black, melanin was widely distributed in one side of the middle fold and the two sides of the outer fold. After L-Tyrosinase feeding, more melanin was found in the groove between the outer fold and the middle fold of black shell oyster.

Concentration Analysis of cAMP, DA, NA, and EPI

cAMP is regarded as a crucial messenger in the control of pigmentation in some vertebrates. It functions as an intracellular second messenger to activate CREB/CREM that activates MITF and induces melanogenesis. As is shown in Fig. 6A, the concentration of cAMP in black shell oyster were significantly higher than in white shell oyster ($P < 0.01$). A substantial rise in cAMP level was seen in black shell oysters following L-Tyrosine feeding ($P < 0.01$), while that change in white shell oysters was not significant.

DA, EPI, and NA are intermediates of tyrosine metabolism and are potential activators in the cAMP signaling pathway. According to Fig. 6B, the DA level was higher in black shell oysters than in white, but the difference was not significant. However, after L-Tyrosinase feeding, the difference became significant ($P < 0.01$). The concentration of NA was lower in black than in white shell oysters ($P < 0.01$) (Fig. 6C) and it dramatically increased in black shell oysters after L-Tyrosinase feeding ($P < 0.01$). There

were no significant differences in EPI levels between black and white shell oysters (Fig. 6D). After L-Tyrosinase feeding, no significant difference was observed in EPI levels in both black and white shell oysters.

Cell Culture and L-Tyrosine Incubation Assay

In this study, an L-Tyrosine incubation experiment was conducted to identify the interaction of the cAMP pathway and tyrosine metabolism and melanin synthesis in *C. gigas*. After incubation with L-Tyrosine, the expression of cAMP and Melanogenesis pathway genes (*PKA, PRKAR, CREM,*

Table 1 Validation of RNA-Seq results using the qPCR method

Group	Gene ID	Abbreviation	Log2 fold change	
			RNA-seq	qPCR
TB vs. CB	LOC105340585	*ADCY1*	−1.1	−0.9
	LOC117680611	*ABCC4-0611*	1.2	2.3
	LOC105328996	*HTR4-8996*	−1.5	−1.7
	LOC105344040	*TYRP2-4040*	1.9	2.1
	LOC105337069	*EIF2AK4*	−1.3	−1.0
	LOC105342404	*TBH-2404*	1.3	1.5
	LOC105318244	*TYRP-8244*	1.5	1.6
	LOC105331837	*PER-1837*	2.5	1.3
	LOC105326074	*SLC22A14*	1.5	2.1
TW vs. CW	LOC105326628	*GPROAR1*	1.1	1.5
	LOC105340585	*ADCY1*	−1.1	−1.3
	LOC105327938	*MC4R*	1.6	1.6
	LOC117688080	*TBH-8080*	3.9	2.5
	LOC105320937	*DDC*	−1.9	−1.6
	LOC105318244	*TYRP-8244*	−1.2	−1.1
	LOC105331837	*PER-1837*	−4.1	−4.4
CB vs. CW	LOC105344201	*ADCY10*	−2.0	0.3
	LOC105327938	*MC4R*	1.0	0.5
	LOC105328996	*HTR4-8996*	1.6	2.0
	LOC117688080	*TBH-8080*	2.4	3.1
	LOC105332956	*TYRP1-2956*	2.1	1.0
	LOC105337069	*EIF2AK4*	9.0	5.0
	LOC105331837	*PER-1837*	−2.4	−1.9
TB vs. TW	LOC105326628	*GPROAR1*	−1.5	−1.2
	LOC105344201	*ADCY10*	−1.4	−1.7
	LOC105327938	*MC4R*	−1.1	−1.1
	LOC117680611	*ABCC4-0611*	1.2	2.5
	LOC105344040	*TYRP2-4040*	2.2	2.1
	LOC105332956	*TYRP1-2956*	2.7	1.7
	LOC105337069	*EIF2AK4*	6.6	4.0
	LOC105320937	*DDC*	2.5	2.0
	LOC105318244	*TYRP-8244*	2.6	2.2
	LOC105331837	*PER-1837*	4.2	2.8
	LOC105326074	*SLC22A14*	1.6	1.1

Fig. 5 Tyrosinase activity (**A**) and melanin content (**B**) analysis. Data represents as the mean ± SD (n = 3). The * represents P < 0.05 and ** indicates P < 0.01. **C** The distribution of melanin in the edge mantle in four groups (CB, CW, TB, TW). The middle fold (mf), outer fold (of), inner fold (if), and ganglion (g). Red arrows indicate the location of melanin distribution
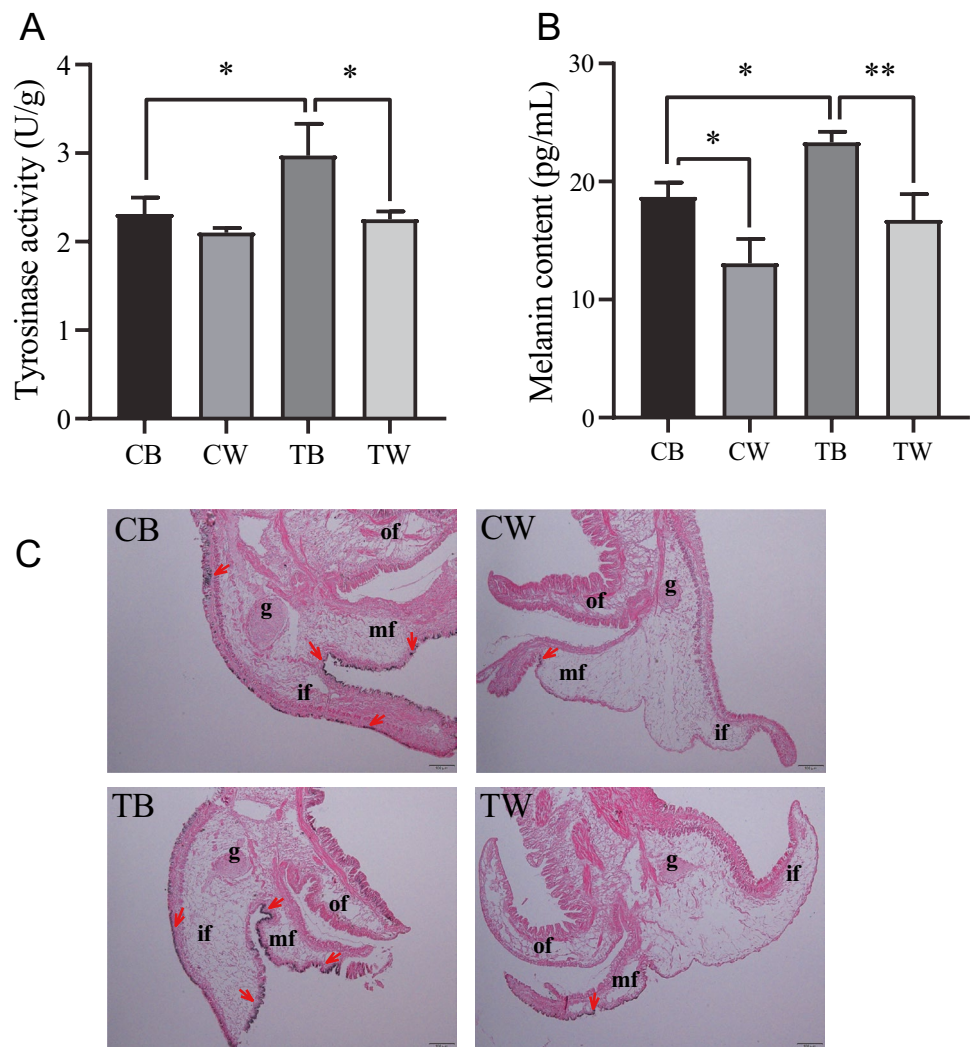
CREB3L2, CREB3L3, CBP, MITF, TYR, and *TYRP*) were detected. Those genes and proteins were upregulated with the increasing concentration (2–100 μM) of L-Tyrosine (Fig. 7A and B). After L-Tyrosine incubation (10 μM), the tyrosinase activity and melanin content increased (Fig. 7C and D). Consist with them, the cAMP level also was significantly upregulated (Fig. 7E). Besides, we found the DA level was remarkably increased after incubation with 2–100 μM L-Tyrosine, but it decreased at 500 μM (Fig. 7F). NA level only upregulated under 2 μM L-Tyrosine and decreased at 100–500 μM of L-Tyrosine (Fig. 7G). The EPI level has not significantly increased under L-Tyrosine incubation and decreased at 500 μM L-Tyrosine (Fig. 7H).

Discussion

In the past decade, several shell color strains of *C. giga* have been developed through selective breeding (Xing et al. 2018; Xu et al. 2019a; Han et al. 2020). Those strains provide excellent materials for the study of melanin synthesis and shell color formation. Oyster mantle plays an important role in shell growth and shell color formation (Brake et al. 2004). It could be divided into the central mantle and edge mantle, the latter has three folds, outer, middle, and inner folds. The central mantle is mainly involved in mineralization and the formation of the nacreous shell layer (Aguilera et al. 2014), and the edge mantle is responsible for shell color formation (Zhu et al. 2022). In this study, we compared the difference in the edge mantle transcriptome of black and white shell oysters before and after L-Tyrosine feeding.

Some pigment-related genes (*TYR, TYRP, DBH, TBH, HTR4, ANPRA, MC4R*, and *CRHR2*) were found differentially expressed in the black and white shell oyster strains. *TYR* and *TYRP* are rate-limiting enzymes in tyrosine metabolism and melanin synthesis, which have been identified in many molluscans (Yu et al. 2018). In *C. gigas*, the knockdown *CgTyp-1* or *CgTyp-3* decreased tyrosinase activity and the number of melanosomes in the outer fold of the mantle (Zhu et al. 2022). *TYRP1* involves in the survival

Fig. 6 ELISA analysis of **A** cAMP, **B** DA, **C** NA, and **D** EPI level before and after L-Tyrosine feeding. Data represents as the mean ± SD ($n = 3$). The * represents $P < 0.05$, ** indicates $P < 0.01$, and ns represents not significant
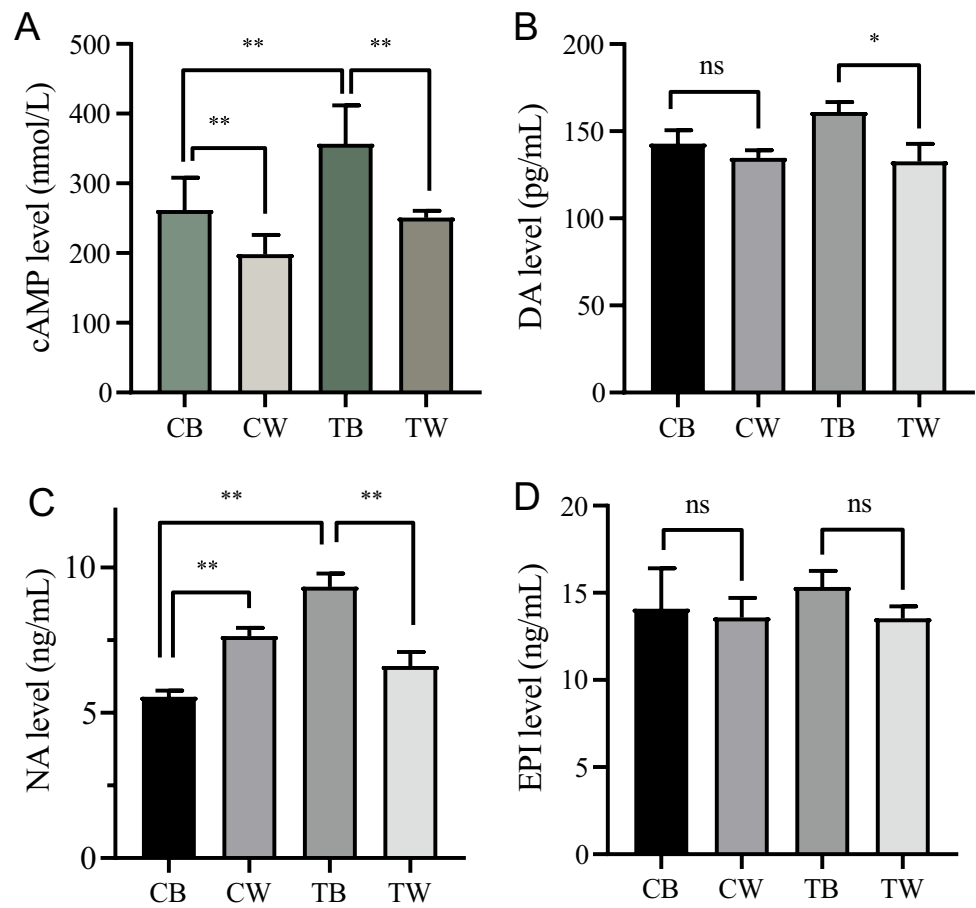
and proliferation of melanocytes and plays a role in converting Dopaquinone to melanin polymer (Del Marmol and Beermann 1996; Bian et al. 2021). We also found the tyrosinase activity and melanin content in black shell oysters were higher than in white (Fig. 5). L-Tyrosine feeding dramatically increased tyrosinase activity and melanin content in the black shell oyster, but no significant change in the white (Fig. 5). Those results indicate a variation in melanin synthesis and tyrosine metabolism in these two shell color strains.

L-Tyrosine serves as a precursor to the melanin pigment, catecholamines, tyramine/octopamine, and thyroid hormones (Slominski et al. 2012) and is often used as a dietary supplement to improve body color (Wang et al. 2018). In this study, more DEGs were identified between the two shell color strains after L-Tyrosine feeding. Some important genes were significantly regulated in black shell *C. gigas*, such as *VPS13*, *BMP2*, *BMP4*, *DDC*, and *OCA2*. VPS proteins are mainly responsible for the sorting and delivery of soluble vacuoles (Song and Wang 2021). Recently, several studies have proven VPS plays an important role in pigment accumulation (Clancey et al. 2013; Song and Wang 2021). *VPS13* genes were found to interact with melanophore survival and

density in red tilapia (Fang et al. 2022). In scallops, *VPS29* functions as an important regulator in carotenoid-induced coloration (Song and Wang 2021). *DDC* catalyzes the decarboxylation of DOPA to Dopamine, which plays a crucial role in Dopamine-melanin synthesis in insects (Chen et al. 2019). Silencing DDC in third-instar larvae of *Harmonia axyridis* resulted in an abnormal phenotype with decreased elytra melanin (Chen et al. 2019). The upregulated *DDC* gene expression in the black shell oysters implies the difference in L-Tyrosine metabolism and melanin synthesis in the two shell color strains. Our findings indicate a potential role of *VPS13* and *DDC* genes in oyster tyrosine metabolism and melanogenesis. *OCA2*, also known as P protein, is a 12-pass membrane protein that has been suggested to modulate melanosome pH and transport L-Tyrosine and Tyrosinase (Bilandžija et al. 2013; McCauley et al. 2016). In *Pinctada margaritifera,* an *OCA2* gene downregulated in the albino phenotype mantle of *P. margaritifera* (Auffret et al. 2020). In our result, *OCA2* expression was significantly higher in the white than the black before and after L-Tyrosine feeding. This finding is opposite to some previous research. The upregulated expression of OCA2 in the white shell oyster
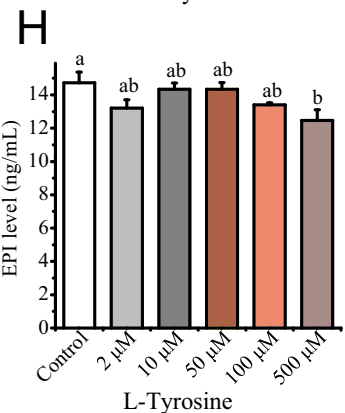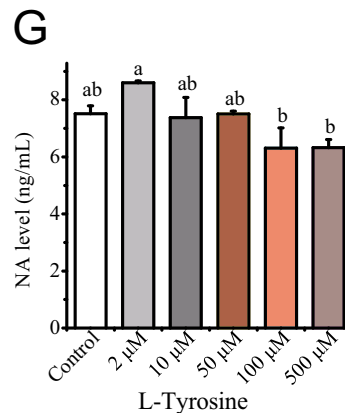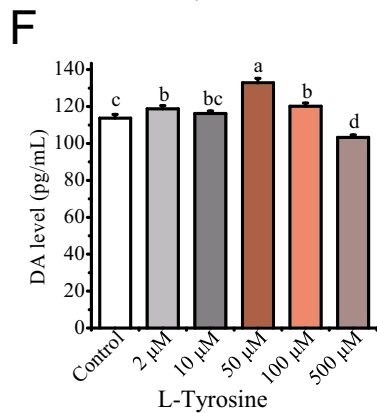
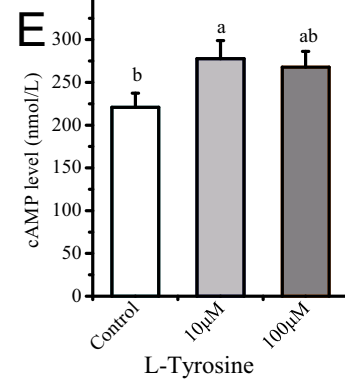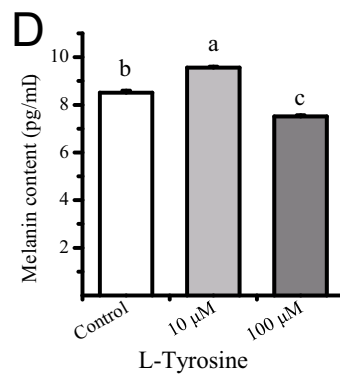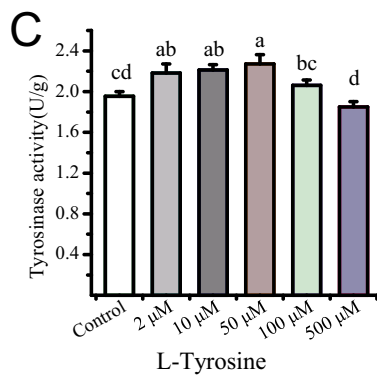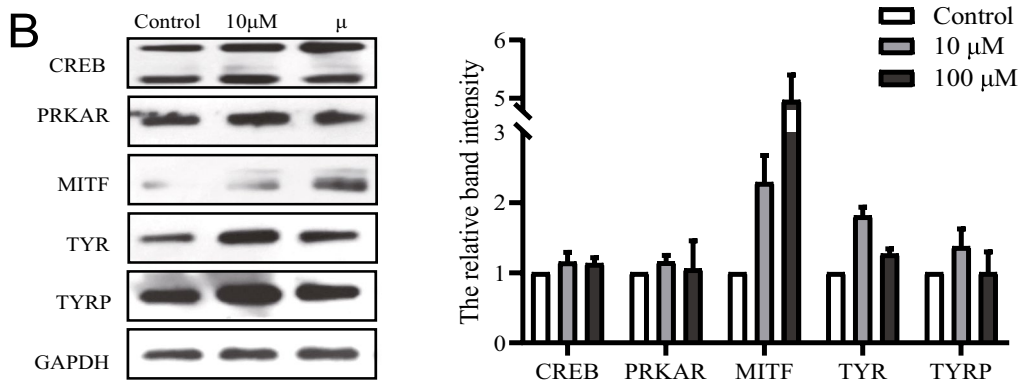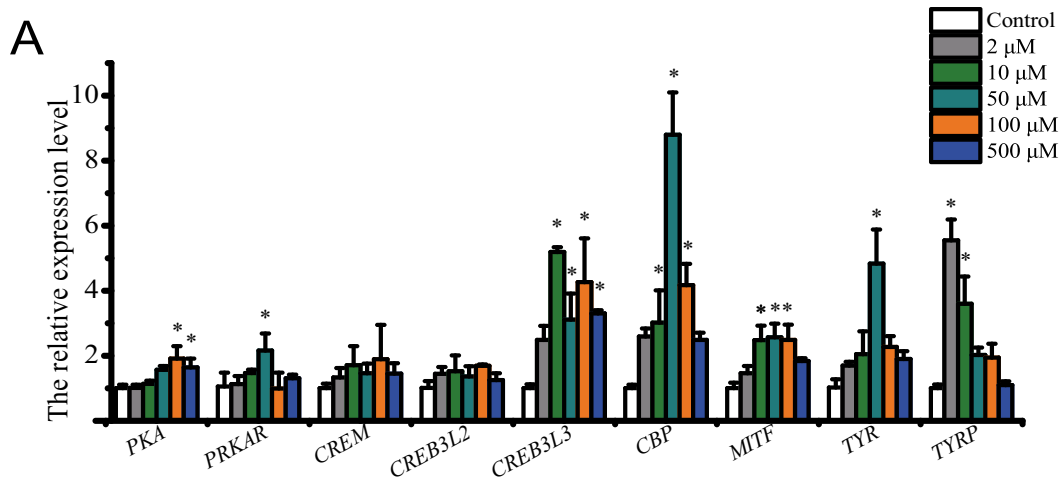◄**Fig. 7** Mantle cell culture and ʟ-Tyrosine incubation assays. **A** qPCR analysis of the relative expression level of genes (from cAMP-mediated melanogenesis pathway) in the mantle cells of black shell oysters after ʟ-Tyrosine incubation. **B** Western blot analysis of CREB, PRKAR, MITF, TYR, and TYRP after ʟ-Tyrosine incubation. GAPDH was used as an internal reference. The blotting band intensity was determined using ImageJ software. **C** Tyrosinase activity and **D** melanin content analysis in mantle cells after ʟ-Tyrosine incubation. **E** The cAMP level in mantle cells after ʟ-Tyrosine incubation. **F** DA, **G** NA, and **H** EPI content analysis after ʟ-Tyrosine incubation with different concentrations. Data represents as the mean $\pm$ SD ($n=3$). The * represents $P < 0.05$. Bars with different letters indicate significant differences ($P < 0.05$) between groups

may be to compensate for the functional defects (Sun et al. 2016). We speculate that the relatively higher expression of the OCA2 gene in the white shell oysters is associated with the defect of tyrosine metabolism and melanin synthesis.

Several pathways related to tyrosine metabolism and melanin synthesis were found in the present study (Fig. 2). Retinol metabolism and Cytochrome P450 pathways were reported to interact with melanin biosynthesis by catalyzing retinoate into retinoic acid (Yu et al. 2017). Retinoic acid is a metabolic intermediate product of vitamin A, mainly affecting growth and promoting cell proliferation, differentiation, and other metabolic effects (Albalat 2009). High concentration of retinoic acid affects the shell structure and arrest development at the trochophore stage in molluscs (Albalat 2009). According to the report of Jin et al. (2022), all-trans retinoic acid could activate *CgTYR* expression. Retinoic acid receptor (*Cg*RAR) regulates Tyr-2 transcriptional expression, which contributes to melanin production. Cytochrome P450 is participate in pheomelanin synthesis and pigment accumulation in some bivalves (Yu et al. 2017; Song and Wang 2019). It was reported that CYP450 plays an important role in the formation of orange coloration by accumulating different pigments in scallops (Song and Wang 2019). In *C. gigas*, a CYP450 gene implicates the production of melanin and carotenoid and is negatively regulated by a microRNA dme-miR-1-3p (Li et al. 2021b). According to Yu et al. (2017), Cytochrome P450 genes were upregulated in the black *C. gigas* mantle and adductor muscle. Those results support that CYP450 and Retinol metabolism could affect retinoic acid production, increase tyrosinase activity, and produce melanin in *C. gigas*.

After ʟ-Tyrosine feeding, Melanogenesis and Tyrosine metabolism pathways were enriched in TB vs TW groups. The Melanogenesis pathway has been well investigated in some vertebrates. The key regulatory pathways, SCF/KIT, Wnt/β- catenin, MAPK, and cAMP, were identified in the process of melanogenesis in fish (Luo et al. 2021). In the Melanogenesis pathway, MITF plays an important role that aggregates signals from all upstream pathways and mediates tyrosine metabolism and melanin synthesis by downstream

tyrosinase family genes. The process of tyrosine metabolism is different between invertebrates and mammals (Vavricka et al. 2014). Compared with mammals, invertebrates have more homologous enzymes involved in tyrosine metabolism. In that process, Tyrosine is hydroxylated to ʟ-DOPA which can directly involve in melanin production, or be catalyzed by DDC to Dopamine, then Dopamine continues to produce norepinephrine by the action of DOPA hydroxylase (Alberto et al. 2011; Sun et al. 2017).

The cAMP signaling pathway is known to regulate metabolism, secretion, calcium homeostasis, muscle contraction, cell fate, and gene transcription (Schmidt et al. 2013). This pathway involved in pigment has been well investigated in some fish (Yamanome et al. 2007; Luo et al. 2019). In barfin flounder, the melanocyte-stimulating hormone (MSH) peptide increases intracellular cAMP levels and activates protein kinase A (PKA) thus inducing tyrosinase enzyme activation to produce melanin (Yamanome et al. 2007). A long non-coding RNA and mRNA sequencing analysis revealed cAMP signaling, melanogenesis, and tyrosine metabolism appear to affect the skin pigmentation of Koi carp (*Cyprinus carpio* L.) (Luo et al. 2019). Here, the cAMP signaling pathway was enriched in CB vs. CW and TB vs TW groups. The integrated analysis presented the association between cAMP and the melanogenesis pathway (Fig. 3). Our results suggest a potential role of the cAMP signaling pathway in melanin synthesis and tyrosine metabolism in *C. gigas.*

cAMP is a key messenger in the regulation of skin pigmentation (Bertolotto et al. 2001). It activates a melanocyte-specific pathway and regulates the activity of melanogenic enzymes (Otręba et al. 2012). In the present study, the cAMP level was significantly higher in the black shell oyster than in the white (Fig. 6). The expression of genes in the cAMP-mediated melanogenesis pathway including *MC4R*, *ADCY1*, *PKA*, *CREM*, *MITF*, *TYR*, and *TYPR* also was higher in the black shell oysters than the whites (Fig. 4). The level of cAMP significantly increased and was consistent with the upregulated expression of *MITF*, *TYR*, and *TYPR* in the black shell oysters after ʟ-Tyrosine feeding. It has been reported that an elevated level of intracellular cAMP activates CREB leading to an increase in the expression of MITF and melanogenic enzymes (Kim et al. 2015; Sun et al. 2017). The in vitro incubation assays showed that these gene and protein expressions (*CREM*, *CREB, CBP, MITF, TYR*, and *TYR*) also increased following the upregulated cAMP levels in oyster mantle cells (Fig. 7). Those results imply a cAMP-mediated melanogenesis pathway might regulate tyrosine metabolism and melanin synthesis in *C. gigas.*

DA and NA are metabolites of tyrosine metabolism as well as signaling molecules of the cAMP signaling pathway (Florou et al. 2012). They activate AC through GPCR, then AC converts ATP to cAMP and regulates downstream gene expression. Our result revealed that the

NA level of black shell oysters is significantly higher than that of white shell oysters (Fig. 6). Besides, after L-tyrosine feeding, the level of DA, and NA dramatically increased in black shell oysters while no significant changes in white shell oysters. The in vitro incubation assays showed that tyrosinase activity and melanin content also increased following the increase of cAMP, DA, and NA levels. Our results indicate DA and NA might function as feedback regulators and participate in the cAMP-mediated melanogenesis pathway. Interestingly, this regulatory mode seems more active in the black shell oyster since not only the level of cAMP, DA, and NA but also the expression of genes in the cAMP-mediated melanogenesis pathway showed a higher level in the black than the white. We presume that a cAMP-mediated melanogenesis pathway might regulate pigmentation and shell color formation in *C. gigas*.

Conclusion

In this study, we compared the mantle transcriptome of black and white shell strains of *C. gigas* based on L-Tyrosine feeding. Several key regulatory pathways involved in tyrosine metabolism and melanin synthesis were found, including Cytochrome P450, melanogenesis, tyrosine metabolism, and the cAMP signaling pathway. Most DEGs in those pathways exhibited a higher expression in the black shell oyster than in the white indicating the difference in gene expression may cause the variation of tyrosine metabolism and melanin synthesis in black and white shell *C. gigas*. Through the transcriptomic and physiological analysis, we found the important roles of cAMP in the regulation of tyrosine metabolism and melanin synthesis in oysters. The present study not only reveals the difference in tyrosine metabolism and melanin synthesis in black and white shell oysters but also provides evidence for cAMP-mediated melanogenesis regulating shell color formation in *C. gigas*.

Author Contributions Kunyin Jiang: completion of the experiment, data analysis, and manuscript drafting. Qi Li: experimental design and coordination, manuscript revision, and funding acquisition. Chengxun Xu: resources. Hong Yu: resources. Lingfeng Kong: resources. Shikai Liu: investigation.

Data Availability The transcriptome data have been deposited in the Sequence Read Archive (SRA) database with the accession number PRJNA900369 (https://www.ncbi.nlm.nih.gov/bioproject/PRJNA900369).

Declarations

Ethics Approval The *C. gigas* used in this study are neither an endangered nor protected species. All experiments in this study were conducted according to national and institutional guidelines.

Conflict of Interest The authors declare no competing interests.

References

Aguilera F, McDougall C, Degnan BM (2014) Evolution of the tyrosinase gene family in bivalve molluscs: independent expansion of the mantle gene repertoire. Acta Biomater 10:3855–3865

Albalat R (2009) The retinoic acid machinery in invertebrates: ancestral elements and vertebrate innovations. Mol Cell Endocrinol 313:23–35

Alberto CO, Trask RB, Hirasawa M (2011) Dopamine acts as a partial agonist for α2A adrenoceptor in melanin-concentrating hormone neurons. J Neurosci 31:10671–10676

Auffret P, Le Luyer J, Sham Koua M, Quillien V, Ky CL (2020) Tracing key genes associated with the *Pinctada margaritifera* albino phenotype from juvenile to cultured pearl harvest stages using multiple whole transcriptome sequencing. BMC Genomics 21:1–14

Bandaranayake WM (2006) The nature and role of pigments of marine invertebrates. Nat Prod Rep 23:223–255

Barnard W, De Waal D (2006) Raman investigation of pigmentary molecules in the molluscan biogenic matrix. J Raman Spectrosc 37:342–352

Bertolotto C, Busca R, Ballotti R, Ortonne JP (2001) Cyclic AMP is a key messenger in the regulation of skin pigmentation. Medecine/sciences 17:177–185

Bian C, Li R, Wen Z, Ge W, Shi Q (2021) Phylogenetic analysis of core melanin synthesis genes provides novel insights into the molecular basis of albinism in fish. Front Genet 12:1–9

Bilandžija H, Ma L, Parkhurst A, Jeffery WR (2013) A potential benefit of albinism in Astyanax Cavefish: downregulation of the oca2 gene increases tyrosine and catecholamine levels as an alternative to melanin synthesis. PLoS One 8:e80823

Boettiger A, Ermentrout B, Oster G (2009) The neural origins of shell structure and pattern in aquatic mollusks. Proc Natl Acad Sci 106:6837–6842

Brake J, Evans F, Langdon C (2004) Evidence for genetic control of pigmentation of shell and mantle edge in selected families of Pacific oysters, *Crassostrea gigas*. Aquaculture 229:89–98

Chen X, Xiao D, Du X, Guo X, Zhang F, Desneux N, Zang L, Wang S (2019) The role of the dopamine melanin pathway in the ontogeny of elytral melanization in *Harmonia axyridis*. Front Physiol 10:1–8

Chen M, Liu B, Ma B, Liu G, Cao W, Liu X, Yan X, Yang B, Wang C (2020) Selection of a carotenoid-rich scallop strain, QN Orange, from the inter-specific hybrids between the bay scallop and the Peruvian scallop. Aquaculture 528:735513

Clancey LF, Beirl AJ, Linbo TH, Cooper CD (2013) Maintenance of melanophore morphology and survival is cathepsin and vps11 dependent in zebrafish. PLoS ONE 8:e65096

Del Marmol V, Beermann F (1996) Tyrosinase and related proteins in mammalian pigmentation. FEBS Lett 381:165–168

Fang W, Huang J, Li S, Lu J (2022) Identification of pigment genes (melanin, carotenoid and pteridine) associated with skin color variant in red tilapia using transcriptome analysis. Aquaculture 547:737429

Florou D, Scorilas A, Vassilacopoulou D, Fragoulis E (2012) DDC (dopa decarboxylase (aromatic L-amino acid decarboxylase)). Atlas Genet Cytogenet Oncol Haematol 14:942–950

Fu L, Shi H, Dai W, Yao H, Bao Y, Lin Z, Dong Y (2021) Characterization and function analysis of β, β-carotene-9′, 10′-oxygenase 2 (BCDO2) gene in carotenoid metabolism of the red shell hard clam (*Meretrix meretrix*). Front Mar Sci 8:746026

Ge J, Li Q, Yu H, Kong L (2014) Identification and mapping of a SCAR marker linked to a locus involved in shell pigmentation of the Pacific oyster (*Crassostrea gigas*). Aquaculture 434:249–253

Ge J, Li Q, Yu H, Kong L (2015) Mendelian inheritance of golden shell color in the Pacific oyster *Crassostrea gigas*. Aquaculture 441:21–24

Grant HE, Williams ST (2018) Phylogenetic distribution of shell colour in Bivalvia (Mollusca). Biol J Linn Soc 125:377–391

Guo X (2009) Use and exchange of genetic resources in molluscan aquaculture. Rev Aquac 1:251–259

Han Z, Li Q, Liu S, Kong L (2020) Crossbreeding of three different shell color lines in the Pacific oyster reveals high heterosis for survival but low heterosis for growth. Aquaculture 529:735621

Hoang TH, Qin JG, Stone DAJ, Harris JO, Duong DN, Bansemer MS (2016) Colour changes of greenlip abalone (*Haliotis laevigata* Donovan) fed fresh macroalgae and dried algal supplement. Aquaculture 456:16–23

Huang S, Jiang H, Zhang L, Gu Q, Wang W, Wen Y, Luo F, Jin W, Cao X (2021) Integrated proteomic and transcriptomic analysis reveals that polymorphic shell colors vary with melanin synthesis in *Bellamya purificata* snail. J Proteomics 230:103950

Irion U, Singh AP, Nüsslein-Volhard C (2016) The developmental genetics of vertebrate color pattern formation: lessons from zebrafish. Curr Top Dev Biol 117:141–169

Jin Q, Huo C, Yang W, Jin K, Cai S, Zheng Y, Huang B, Wei L, Zhang M, Han Y, Zhang X, Liu Y, Wang X (2022) Regulation of tyrosinase gene expression by retinoic acid pathway in the Pacific oyster *Crassostrea gigas*. Int J Mol Sci 23:12840

Kim HJ, Kim JS, Woo JT, Lee IS, Cha BY (2015) Hyperpigmentation mechanism of methyl 3,5-di-caffeoylquinate through activation of p38 and MITF induction of tyrosinase. Acta Biochim Biophys Sin (shanghai) 47:548–556

Li Y, Ren L, Fu H, Yang B, Tian J, Li Q, Liu Z, Liu S (2021a) Crosstalk between dopamine and insulin signaling in growth control of the oyster. Gen Comp Endocrinol 313:1–9

Li Z, Li Q, Liu S, Han Z, Kong L, Yu H (2021b) Integrated analysis of coding genes and non-coding RNAs associated with shell color in the Pacific oyster (*Crassostrea gigas*). Mar Biotechnol 23:417–429

Li Z, Li Q, Xu C, Yu H (2022) Molecular characterization of Pax7 and its role in melanin synthesis in *Crassostrea gigas*. Comp Biochem Physiol Part B Biochem Mol Biol 260:110720

Li Z, Hu B, Du L, Hou C, Qi Li (2023a) Involvement of B-aat1 and Cbs in regulating mantle pigmentation in the Pacific oyster (*Crassostrea gigas*). Mol Biol Rep 50:377–387

Li Z, Xu C, Yu H, Kong L, Liu S, Li Q (2023b) Transcription factor CgPOU3F4-like regulates expression of pheomelanin synthesis related gene CgB-aat1 in the Pacific oyster (*Crassostrea gigas*). Gene 861:147258

Lister JA, Robertson CP, Lepage T, Johnson SL, Raible DW (1999) Nacre encodes a zebrafish microphthalmia-related protein that regulates neural-crest-derived pigment cell fate. Development 126:3757–3767

Luo M, Wang L, Yin H, Zhu W, Fu J, Dong Z (2019) Integrated analysis of long non-coding RNA and mRNA expression in different colored skin of koi carp. BMC Genomics 20:515

Luo M, Lu G, Yin H, Wang L, Atuganile M, Dong Z (2021) Fish pigmentation and coloration: molecular mechanisms and aquaculture perspectives. Rev Aquac 13:2395–2412

McCauley DW, Hixon E, Jeffery WR (2016) Evolution of pigment cell regression in the cavefish Astyanax: a late step in melanogenesis. Evol Dev 6:209–218

Nie H, Jiang K, Jiang L, Huo Z, Ding J, Yan X (2020) Transcriptome analysis reveals the pigmentation related genes in four different shell color strains of the Manila clam *Ruditapes philippinarum*. Genomics 112:2011–2020

Otręba M, Rok J, Buszman E, Wrześniok D (2012) Regulacja melanogenezy: Rola camp i mitf. Postepy Hig Med Dosw 66:33–40

Potts RWA, Gutierrez AP, Cortés-Araya Y, Houston RD, Bean TP (2020) Developments in marine invertebrate primary culture reveal novel cell morphologies in the model bivalve *Crassostrea gigas*. PeerJ 2020:e9180

Saenko SV, Schilthuizen M (2021) Evo-devo of shell colour in gastropods and bivalves. Curr Opin Genet Dev 69:1–5

Schmidt M, Dekker FJ, Maarsingh H (2013) Exchange protein directly activated by cAMP (epac): a multidomain camp mediator in the regulation of diverse biological functions. Pharmacol Rev 65:670–709

Slominski A, Paus R (1994) Towards defining receptors for l-tyrosine and l-DOPA. Mol Cell Endocrinol 99:1987–1991

Slominski A, Tobin DJ, Shibahara S, Wortsman J (2004) Melanin pigmentation in mammalian skin and its hormonal regulation. Physiol Rev 84:1155–1228

Slominski A, Zmijewski MA, Pawelek J (2012) L-tyrosine and L-dihydroxyphenylalanine as hormone-like regulators of melanocyte functions. Pigment Cell Melanoma Res 25:14–27

Song J, Wang C (2019) Transcriptomic and proteomic analyses of genetic factors influencing adductor muscle coloration in QN Orange scallops. BMC Genomics 20:1–10

Song J, Wang C (2021) Transcriptomic and metabonomic analyses reveal roles of VPS 29 in carotenoid accumulation in adductor muscles of QN Orange scallops. Genomics 113:2839–2846

Sun X, Liu Z, Zhou L, Wu B, Dong Y, Yang A (2016) Integration of next generation sequencing and EPR analysis to uncover molecular mechanism underlying shell color variation in scallops. PLoS ONE 11:e0161876

Sun L, Guo Y, Zhang Y, Zhuang Y (2017) Antioxidant and antityrosinase activities of phenolic extracts from rape bee pollen and inhibitory melanogenesis by cAMP/MITF/TYR pathway in B16 mouse melanoma cells. Front Pharmacol 8:1–9

Toews DPL, Hofmeister NR, Taylor SA (2017) The evolution and genetics of carotenoid processing in animals. Trends Genet 33:171–182

Vavricka CJ, Han Q, Mehere P, Ding H, Christensen BM, Li J (2014) Tyrosine metabolic enzymes from insects and mammals: a comparative perspective. Insect Sci 21:13–19

Wang L, Zhu W, Yang J, Miao L, Dong J, Song F, Dong Z (2018) Effects of dietary cystine and tyrosine on melanogenesis pathways involved in skin color differentiation of Malaysian red tilapia. Aquaculture 490:149–155

Wang X, Ding S, Yin D et al (2020) Response to selection for growth in the second generation of two shell color lines of the bay scallop *Argopecten irradians*. Aquaculture 528:735536

Williams ST (2017) Molluscan shell colour. Biol Rev 92:1039–1058

Williams ST, Ito S, Wakamatsu K, Goral T, Edwards NP, Wogelius RA, Henkel T, de Oliveira LFC, Maia LF, Strekopytov S, Jeffries T, Speiser DI, Marsden JT (2016) Identification of shell colour pigments in marine snails *Clanculus pharaonius* and *C. margaritarius* (Trochoidea; gastropoda). PLoS One 11:1–25

Xing D, Li Q, Kong L, Yu H (2018) Heritability estimate for mantle edge pigmentation and correlation with shell pigmentation in the white-shell strain of Pacific oyster, *Crassostrea gigas*. Aquaculture 482:73–77

Xing D, Li Q, Zhang J (2019) Genotype by environment (G×E) interaction for growth and shell color traits in the white-shell strain of Pacific oyster (*Crassostrea gigas*). J Fish China 43:474–482

Xu C, Li Q, Chong J, Liu S, Kong L (2019a) Mass selection for growth improvement in black shell line of Pacific oyster *Crassostrea gigas*. J Ocean Univ China 18:1411–1416

Xu C, Li Q, Yu H, Liu S, Kong L, Chong J (2019b) Inheritance of shell pigmentation in Pacific oyster *Crassostrea gigas*. Aquaculture 512:734249

Yamanome T, Chiba H, Takahashi A (2007) Melanocyte-stimulating hormone facilitates hypermelanosis on the non-eyed side of the barfin flounder, a pleuronectiform fish. Aquaculture 270:505–511

Yan X, Nie H, Huo Z et al (2019) Clam genome sequence clarifies the molecular basis of its benthic adaptation and extraordinary shell color diversity. iScience 19:1225–1237

Yu W, He C, Cai Z, Xu F, Wei L, Chen J, Jiang Q, Wei N, Li Z, Guo W, Wang X (2017) A preliminary study on the pattern, the physiological bases and the molecular mechanism of the adductor muscle scar pigmentation in pacific oyster *Crassostrea gigas*. Front Physiol 8:1–11

Yu F, Qu B, Lin D, Deng Y, Huang R, Zhong Z (2018) Pax3 gene regulated melanin synthesis by tyrosinase pathway in *Pteria penguin*. Int J Mol Sci 19:3700

Yue X, Nie Q, Xiao G, Liu B (2015) Transcriptome analysis of shell color-related genes in the clam *Meretrix meretrix*. Mar Biotechnol 17:364–374

Zhang G, Zhang W, Ye R, Fang A, Ren G, Zheng R, Yang S (2016) Analysis of selective breeding of nacre color in two strains of *Hyriopsis cumingii* Lea based on the cielab colorspace. J Shellfish Res 35:225–229

Zhu Y, Li Q, Yu H, Liu S, Kong L (2021) Shell biosynthesis and pigmentation as revealed by the expression of Tyrosinase and Tyrosinase-like protein genes in Pacific oyster (*Crassostrea gigas*) with different shell colors. Mar Biotechnol 23:777–789

Zhu Y, Li Q, Yu H, Liu S, Kong L (2022) Expression of tyrosinase-like protein genes and their functional analysis in melanin synthesis of Pacific oyster (*Crassostrea gigas*). Gene 840:1–9